

Research on GFSINS/Star-sensor Integrated Attitude Estimation Algorithm Based on UKF

Minghong Zhu, Fei Yu*, Shu Xiao*, and Zhenpeng Wang

Abstract—In this research, an effective nine-accelerometer configuration is designed to form a gyroscope free strapdown inertial navigation system (GFSINS), and the absolute value method is adopted to calculate angular velocity. This paper proposes an UKF attitude estimation algorithm for the star-sensor aided GFSINS integrated navigation system. The experimental results show that, UKF algorithm avoids the higher order truncation error in EKF, and improves the steady-state precision and convergence speed to some extent. Especially in complex models, UKF is free from computational complexity of the Jacobi matrix, thus highlighting the rapidity and improving the computation efficiency of the system. Consequently, this navigation methodology could be competent for some high precision and long-endurance navigation tasks.

Index Terms—GFSINS, star sensor, angular velocity calculation, attitude estimation, UKF.

I. INTRODUCTION

GYROSCOPE free strapdown inertial navigation system (GFSINS) was first proposed by Victor B. Corey in 1962, in which vehicle's angular velocity could be obtained and calculated by specific forces based on the spatial position combination of accelerometers rather than extracted from gyroscopes, and all navigation parameters can be acquired only by accelerometers [1], [2]. Due to the rotating components inside, the gyroscope can not withstand large linear acceleration in traditional strapdown inertial navigation system (SINS) [3]. However, GFSINS can be applied to navigation tasks with large angular acceleration and angular velocity [4]. Furthermore, compared with traditional SINS, GFSINS has the advantages of low cost, low power consumption, long lifetime, fast response, high reliability and strong anti-overload ability [5].

Whether in traditional SINS or GFSINS, there will inevitably be zero drift in accelerometers, and the navigation error will increase with time [6]. Studies offer signs that it is difficult to meet the requirements of navigation with long endurance and high precision [7], [8]. Therefore, a natural approach to design sensors for a system requiring better performance than single SINS may offer, is to fuse the measurements from other navigation devices and SINS to create an artificial high performance integrated navigation system. As the most accurate attitude sensitive instrument at present, star sensor not only can measure attitude angles

with high precision of seconds, but also has the characteristics of strong independence, no attitude accumulation error, unrestricted field-of-view, high anti-interference and good concealment [9], [10]. In this work, the authors implement a GFSINS (core sensor) and star-sensor (aiding sensor) integrated navigation scheme. Specifically, star-sensor observes the stars with known azimuth information to obtain the accurate attitude information, thus correcting the inertial reference error accumulated with time. The combination of two sensors can form an integrated attitude determination system with excellent performance and achieve advantage complementarity.

The advanced filtering estimation method is an effective way to improve the accuracy, instantaneity and reliability of the integrated navigation system and achieve cooperative transcendence, under the condition that the hardware performance of system is certain. EKF is a commonly used nonlinear method, but its performance is affected by the linearization of system and complex calculation of Jacobi matrix [11]. In contrast, UKF transforms the nonlinearity of measurement and state model by unscented transformation (U-transformation for short), thus avoiding the computation of Jacobi matrix and the linearization of state equation and measurement equation, there will be no higher-order truncation error [12]. UKF algorithm, which is utilized in this paper to estimate the attitude angle for GFSINS/star-sensor integrated system, displays more excellent filtering performance than EKF.

In the following, an effective nine-accelerometer configuration is designed to form a gyroscope free strapdown inertial navigation system and the absolute value method is presented to calculate angular velocity in Section II. Attitude estimation algorithm based on UKF for GFSINS/star-sensor integrated system is discussed in Section III. The experimental results demonstrate the advantages of the proposed attitude estimation algorithm based on UKF in Section IV. Conclusions are given in Section V.

II. ACCELEROMETER CONFIGURATION AND ANGULAR VELOCITY CALCULATION OF GFSINS

Different from traditional SINS, the accelerometers must be installed at the noncentraled of the body for GFSINS, only in this way can angular velocity be obtained from the output specific forces of the accelerometers. We fixed m accelerometers on the carrier, and the way to calculate angular velocity is subject to the positions $u_1, u_2, u_3, \dots, u_m$ and sensitive directions $\theta_1, \theta_2, \theta_3, \dots, \theta_m$ of the accelerometers. According to a series of derivations based on Coriolis law, the output of any accelerometer on the carrier could be obtained as follows:

$$f_i = \left[\ddot{R}_i + \Omega \Omega u_i + \dot{\Omega} u_i \right] \cdot \theta_i \quad (1)$$

Manuscript received December 3, 2017; revised September 3, 2018. This work was supported by the National Natural Science Foundation of China under Grant No. 51679047.

M. H. Zhu is with the College of Automation, Harbin Engineering University, Harbin, P.R.China.

F. Yu (Corresponding author) is with the College of Automation, Harbin Engineering University, Harbin, P.R.China (e-mail: yufei414@126.com).

S. Xiao (Corresponding author) is with the College of Automation, Harbin Engineering University, Harbin, P.R.China (e-mail: xsh617@126.com).

Z. P. Wang is with Sichuan Academy of Aerospace Technology, Chengdu, P.R.China.

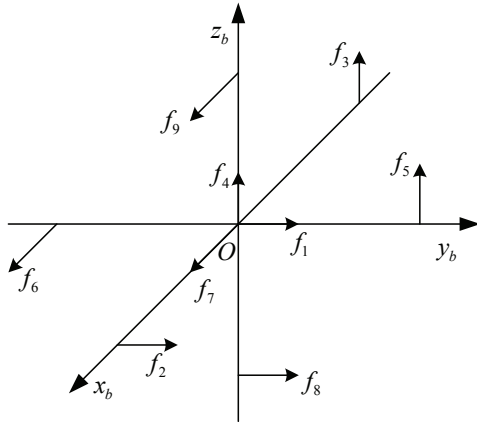


Fig. 1. Nine-accelerometer Configuration Scheme

wherein, \ddot{R}_i is short for $\left. \frac{d^2 R}{dt^2} \right|_i$. Ω is the anti-symmetric matrix of the rotation angular velocity vector ω_{ib}^b .

After further deduction to (1), we can get the following equation:

$$f_i = \left[(u_i \times \theta_i)^T \theta_i^T \right] \begin{bmatrix} \dot{\omega} \\ \mathbf{A} \end{bmatrix} + \theta_i^T \Omega^2 u_i \quad (2)$$

wherein, $\dot{\omega} = [\dot{\omega}_x \ \dot{\omega}_y \ \dot{\omega}_z]^T$ is short for $\dot{\omega}_{ib}^b = [\dot{\omega}_{ibx}^b \ \dot{\omega}_{iby}^b \ \dot{\omega}_{ibz}^b]^T$. f_i represents the output of the i -th accelerometer. u_i represents the position of the i -th accelerometer. θ_i represents the sensitive direction of the i -th accelerometer.

Based on the above principle, an accelerometer configuration is designed for GFSINS. Nine accelerometers are used as inertial measurement units, and the specific force outputs of all accelerometers are $f_1, f_2 \dots f_9$ respectively. The installation mode of each accelerometer in the body frame $O_b X_b Y_b Z_b$ is shown in Fig. 1, then the specific positions and sensitive directions of the nine accelerometers could be expressed as follows:

$$[u_1, \dots, u_9] = l \begin{bmatrix} 0 & 1 & -1 & 0 & 0 & 0 & 0 & 0 & 0 \\ 0 & 0 & 0 & 0 & 1 & -1 & 0 & 0 & 0 \\ 0 & 0 & 0 & 0 & 0 & 0 & 0 & 1 & -1 \end{bmatrix}$$

$$[\theta_1, \dots, \theta_9] = \begin{bmatrix} 0 & 0 & 0 & 0 & 0 & 1 & 1 & 1 & 0 \\ 1 & 1 & 0 & 0 & 0 & 0 & 0 & 0 & 1 \\ 0 & 0 & 1 & 1 & 1 & 0 & 0 & 0 & 0 \end{bmatrix}$$

wherein, l is the distance between the noncentraled accelerometer and the origin of the body frame, the following formula can be obtained as:

$$\left[(u_i \times \theta_i)^T \theta_i^T \right] = \begin{bmatrix} 0 & 0 & 0 & 0 & 1 & 0 \\ 0 & 0 & l & 0 & 1 & 0 \\ 0 & l & 0 & 0 & 0 & 1 \\ 0 & 0 & 0 & 0 & 0 & 1 \\ l & 0 & 0 & 0 & 0 & 1 \\ 0 & 0 & l & 1 & 0 & 0 \\ 0 & 0 & 0 & 1 & 0 & 0 \\ 0 & l & 0 & 1 & 0 & 0 \\ l & 0 & 0 & 0 & 1 & 0 \end{bmatrix}$$

According to (2), the specific force output formula of each

accelerometer can be derived as:

$$\begin{cases} f_1 = A_y \\ f_2 = A_y + l(\dot{\omega}_z + \omega_x \omega_y) \\ f_3 = A_z + l(\dot{\omega}_y - \omega_x \omega_z) \\ f_4 = A_z \\ f_5 = A_z + l(\dot{\omega}_x + \omega_y \omega_z) \\ f_6 = A_x + l(\dot{\omega}_z - \omega_x \omega_y) \\ f_7 = A_x \\ f_8 = A_x + l(\dot{\omega}_y + \omega_x \omega_z) \\ f_9 = A_y + l(\dot{\omega}_x - \omega_y \omega_z) \end{cases} \quad (3)$$

According to (3), the expression of linear acceleration, angular acceleration and the product terms of angular velocity can be arranged as follows:

$$\begin{cases} A_x = f_7 \\ A_y = f_1 \\ A_z = f_4 \end{cases} \quad (4)$$

$$\begin{cases} \dot{\omega}_x = \frac{f_5 + f_9 - f_1 - f_4}{2l} \\ \dot{\omega}_y = \frac{f_3 + f_8 - f_4 - f_7}{2l} \\ \dot{\omega}_z = \frac{f_2 + f_6 - f_1 - f_7}{2l} \end{cases} \quad (5)$$

$$\begin{cases} \omega_x \omega_y = \frac{f_2 + f_7 - f_1 - f_6}{2l} \\ \omega_y \omega_z = \frac{f_1 + f_5 - f_4 - f_9}{2l} \\ \omega_x \omega_z = \frac{f_4 + f_8 - f_3 - f_7}{2l} \end{cases} \quad (6)$$

Equation (7) can be derived from (6) as:

$$\begin{cases} \omega_x^2 = \frac{(f_2 + f_7 - f_1 - f_6)(f_4 + f_8 - f_3 - f_7)}{2l(f_1 + f_5 - f_4 - f_9)} \\ \omega_y^2 = \frac{(f_2 + f_7 - f_1 - f_6)(f_1 + f_5 - f_4 - f_9)}{2l(f_4 + f_8 - f_3 - f_7)} \\ \omega_z^2 = \frac{(f_1 + f_5 - f_4 - f_9)(f_4 + f_8 - f_3 - f_7)}{2l(f_2 + f_7 - f_1 - f_6)} \end{cases} \quad (7)$$

The linear acceleration A_x, A_y, A_z relative to the inertial coordinate frame can be got from (4). The absolute values $|\omega_x|, |\omega_y|, |\omega_z|$ of the angular velocities can be calculated from (7). At the same time, the signs of angular velocities obtained by the integral for (5) are used as the signs of the absolute values of angular velocities. To be specific, the angular velocities $\omega_x, \omega_y, \omega_z$ are expressed as follows:

$$\begin{cases} |\omega_x| = \sqrt{\frac{(f_2 + f_7 - f_1 - f_6)(f_4 + f_8 - f_3 - f_7)}{2l(f_1 + f_5 - f_4 - f_9)}} \\ |\omega_y| = \sqrt{\frac{(f_2 + f_7 - f_1 - f_6)(f_1 + f_5 - f_4 - f_9)}{2l(f_4 + f_8 - f_3 - f_7)}} \\ |\omega_z| = \sqrt{\frac{(f_1 + f_5 - f_4 - f_9)(f_4 + f_8 - f_3 - f_7)}{2l(f_2 + f_7 - f_1 - f_6)}} \end{cases} \quad (8)$$

$$\begin{cases} \omega_x = \text{sign}(\dot{\omega}_x(k+1)) |\omega_x| \\ \omega_y = \text{sign}(\dot{\omega}_y(k+1)) |\omega_y| \\ \omega_z = \text{sign}(\dot{\omega}_z(k+1)) |\omega_z| \end{cases} \quad (9)$$

According to the designed spatial position of nine-accelerometer, the linear acceleration and angular velocity of the carrier could be calculated by using the absolute value method. Thus far, all the parameters required for inertial navigation have been obtained.

III. ATTITUDE ESTIMATION SCHEME DESIGN FOR GFSINS/STAR-SENSOR

The loosely-coupled integration architecture based on the optimal estimation is adopted in this research. The error equation of the gyro-free strapdown inertial device is used as the system state equation. The difference between the attitude from GFSINS and the high precision attitude from star sensor is used as measurement. By using UKF, accelerometer

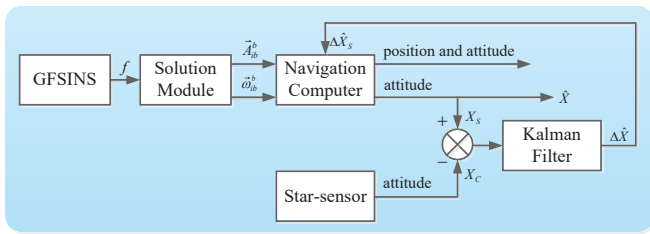


Fig. 2. Loosely-coupled Integration Architecture Based on Optimal Estimation

output error is estimated, to compensate the attitude error of gyro-free strapdown inertial device, and to alleviate a series of calculation errors arise from the accelerometer information solution. During filtering, the estimation of navigation parameter error is fed back to the navigation system to correct the error state. Due to the integration architecture can compensate real-time errors caused by the inertial device and thus improve the accuracy of integrated navigation, it can be applied to long-endurance work. The integration mode is shown in Fig. 2.

A. The Formulation of UKF

UKF is a straightforward application of U-transformation. U-transformation is a method for calculating the statistics of a random variable which undergoes a nonlinear transformation. Based on the principle, it is easier to approximate a probability distribution than an arbitrary nonlinear function. A discrete nonlinear system is assumed as:

$$\begin{cases} x_{k+1} = f(x_k, u_k, k) + \omega_k \\ y_k = h(x_k, u_k, k) + \nu_k \end{cases} \quad (10)$$

wherein, x_k represents the state vector of the system. u_k represents the input control vector. ω_k represents the system noise vector. y_k represents the observation vector. ν_k represents the measurement noise vector.

The following is the general process of U-transformation. Firstly, looking for a series of Sigma points around \hat{x}_k , and the mean and covariance of the sampling points are denoted by \hat{x}_k and P_k respectively. Then searching some Sigma points near $\hat{X}(k|k)$, and the mean and covariance of the selected Sigma points are denoted by $\hat{X}(k|k)$ and $P(k|k)$ respectively. After that, calculating the Sigma points generated by the nonlinear transformation of all sample Sigma points and determining the predicted mean and covariance. Let the state vector be n -dimension. Then the $2n + 1$ Sigma points and their weights are as follows:

$$\begin{cases} \chi_{0,k} = \hat{x}_k & W_0 = \frac{\tau}{(n+\tau)} \\ \chi_{i,k} = \hat{x}_k + \sqrt{n+\tau}(\sqrt{P(k|k)})_i & W_i = \frac{1}{1/[2(n+\tau)]} \\ \chi_{i+n,k} = \hat{x}_k - \sqrt{n+\tau}(\sqrt{P(k|k)})_i & W_{i+n} = \frac{1}{1/[2(n+\tau)]} \end{cases} \quad (11)$$

wherein, $\tau \in R$; when $P(k|k) = A^T A$, $(\sqrt{P(k|k)})_i$ takes the i -th line of A ; and when $P(k|k) = A A^T$, $(\sqrt{P(k|k)})_i$ takes the i -th column of A .

If the state variables are Gaussian distributed and each order of Gaussian distribution can be expressed by the corresponding mean and variance, the relevant parameter values can be determined by theoretical derivation or approximation. If the state variables, except for the initial distribution, cannot satisfy Gaussian distribution even after the transformation of

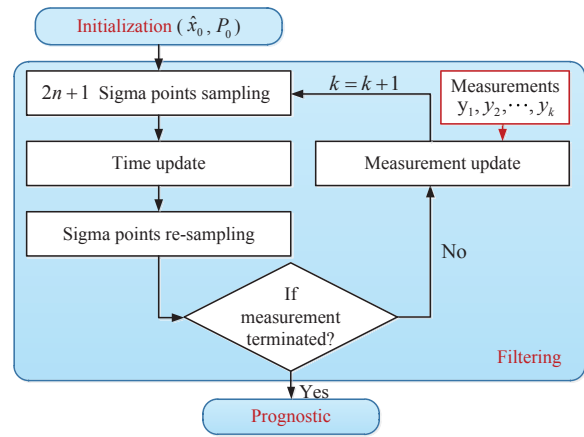


Fig. 3. The Algorithm Flow of UKF

nonlinear functions, we have to adjust each parameter by numerical simulation to get the best filtering performance. The specific algorithm is as follows, and Fig. 3 shows the algorithm flow of UKF.

1) Initialization:

$$\hat{x}_0 = E[x_0], \quad P_0 = E[(x_0 - \hat{x}_0)(x_0 - \hat{x}_0)^T], \quad k \geq 1 \quad (12)$$

2) Computing Sigma Points:

$$\chi_{k-1} = [\hat{x}_{k-1} \hat{x}_{k-1} + \sqrt{n+\tau}(\sqrt{P_{k-1}})_i(\hat{x}_{k-1} - 1)], \quad i = 1, 2, \dots, n \quad (13)$$

3) Time update:

$$\chi_{k|k+1} = f(\chi_{k-1}, u_{k-1}, k-1) \quad (14)$$

$$\hat{x}_k^- = \sum_{i=0}^{2n} W_i \chi_{i,k|k-1} \quad (15)$$

$$P_k^- = \sum W_i [\chi_{i,k|k-1} - \hat{x}_k^-][\chi_{i,k|k-1} - \hat{x}_k^-]^T + Q_k \quad (16)$$

$$y_{k|k-1} = h(\chi_{k|k-1}, u_k, k) \quad (17)$$

$$\hat{y}_k^- = \sum_{i=0}^{2n} W_i y_{i,k|k-1} \quad (18)$$

where, Q_k is the system noise covariance matrix.

4) Measurement update:

$$P_{\hat{y}_k \hat{y}_k} = \sum_{i=0}^{2n} W_i [y_{i,k|k-1} - \hat{y}_k^-][y_{i,k|k-1} - \hat{y}_k^-]^T + R_k \quad (19)$$

$$P_{x_k y_k} = \sum_{i=0}^{2n} W_i [\chi_{i,k|k-1} - \hat{x}_k^-][y_{i,k|k-1} - \hat{y}_k^-]^T \quad (20)$$

$$K_k = P_{x_k y_k} P_{\hat{y}_k \hat{y}_k}^{-1} \quad (21)$$

$$\hat{x}_k = \hat{x}_k^- + K_k (y_k - \hat{y}_k^-) \quad (22)$$

$$P_k = P_k^- - K_k P_{\hat{y}_k \hat{y}_k} K_k^T \quad (23)$$

where, R_k is the measurement noise covariance matrix.

When $x(k)$ is assumed to be Gaussian distributed, $n + \tau = 3$ is usually selected. When $\tau < 0$, the calculated estimation error covariance matrix $P(k + 1|k)$ might be negative. In this case, a modified prediction algorithm is often used, in which (12) is still used to calculate the mean of the predicted value and the covariance of the predicted value is calculated around $\chi_{0,k+1|k}$.

B. The Establishment of State Equation

The attitude precision of star sensor is very advanced. Using Rodrigues parameters as attitude representation, and let Rodrigues parameter be:

$$\sigma = [\sigma_1 \quad \sigma_2 \quad \sigma_3]^T \quad (24)$$

wherein, σ is the Rodrigues parameter of star sensor frame relative to inertial frame. The differential equation of star kinematics is expressed as:

$$\dot{\sigma} = \frac{1}{2}[\omega + \sigma \times \omega + (\sigma \cdot \omega)\sigma] = H(\sigma)\omega \quad (25)$$

with,

$$H(\sigma) = \frac{1}{2} \{I_3 + \hat{\sigma} + \sigma\sigma^T\} \\ = \frac{1}{2} \begin{bmatrix} 1 + \sigma_1^2 & -\sigma_3 + \sigma_1\sigma_2 & \sigma_2 + \sigma_1\sigma_3 \\ \sigma_3 + \sigma_1\sigma_2 & 1 + \sigma_2^2 & -\sigma_1 + \sigma_2\sigma_3 \\ -\sigma_2 + \sigma_1\sigma_3 & \sigma_1 + \sigma_2\sigma_3 & 1 + \sigma_3^2 \end{bmatrix}$$

wherein, $\hat{\sigma}$ is the anti-symmetric matrix of σ , specifically

$$\hat{\sigma} = \begin{bmatrix} 0 & -\sigma_3 & \sigma_2 \\ \sigma_3 & 0 & -\sigma_1 \\ -\sigma_2 & \sigma_1 & 0 \end{bmatrix}$$

Equation (25) is expressed in the form of nonlinear function:

$$\dot{\sigma} = f_1(\sigma, \omega) \quad (26)$$

Based on the integration mode of this research, it is known from attitude kinematics and dynamics:

$$\dot{\omega} = J^{-1} [T_c + T_d - \omega \times (J\omega)] \quad (27)$$

$$T_d = T_{dc} + \Delta T \quad (28)$$

wherein, T_{dc} represents constant disturbance torque. ΔT represents Gaussian white noise, $\Delta T \sim N(0, \sigma_{\Delta T}^2)$.

Then another description of kinetic equation — the expression of nonlinear function is given as:

$$\dot{\omega} = f_2(\omega, T_{dc}, T_c) \quad (29)$$

Let $X = [\sigma^T \quad \omega^T \quad T_{dc}^T]^T$, the state equation of system can be obtained as:

$$\begin{bmatrix} \dot{\sigma}^T \\ \dot{\omega}^T \\ \dot{T}_{dc}^T \end{bmatrix} = \begin{bmatrix} f_1(\sigma, \omega) \\ f_2(\omega, T_{dc}, T_c) \\ 0 \end{bmatrix} + \begin{bmatrix} 0 \\ J^{-1} \\ 0 \end{bmatrix} \Delta T \quad (30)$$

Equation (30) is written as:

$$\dot{X} = f(X) + W \quad (31)$$

Using the above UKF implementation algorithm, the discrete state equation can be derived when sampling time is small enough:

$$\begin{bmatrix} \sigma_k^T \\ \omega_k^T \\ T_{dc,k}^T \end{bmatrix} = \begin{bmatrix} f_1(\sigma_{k-1}, \omega_{k-1}) \\ f_2(\omega_{k-1}, T_{dc,k-1}, T_{c,k-1}) \\ 0 \end{bmatrix} T_s + \\ \begin{bmatrix} \sigma_{k-1}^T \\ \omega_{k-1}^T \\ T_{dc,k-1}^T \end{bmatrix} + \begin{bmatrix} 0 \\ J^{-1} \\ 0 \end{bmatrix} T_s \cdot \Delta T \quad (32)$$

Equation (32) is the UKF state space model after discretization, and can be written as:

$$X_k = X_{k-1} + \int_0^{T_s} f(X, t) dt + W_{k-1} \quad (33)$$

C. The Establishment of Measurement Equation

In Section II, angular velocity is calculated by the specific force signal in GFSINS, and then the tri-axial attitude initial information could be deduced, i.e. pitch angle θ_0 , heading angle ϕ_{G0} and roll angle γ_0 . Correspondingly, another tri-axial attitude information is got from star sensor, i.e. pitch angle θ , heading angle ϕ_G and roll angle γ . Thus the tri-axial attitude error angle δa can be obtained by making differences between the attitudes, as below

$$\delta a = \begin{bmatrix} a_\theta \\ a_{\phi_G} \\ a_\gamma \end{bmatrix} = \begin{bmatrix} \theta - \theta_0 \\ \phi_G - \phi_{G0} \\ \gamma - \gamma_0 \end{bmatrix} \quad (34)$$

As the error equation of attitude for gyro-free strapdown inertial device is based on mathematical platform misalignment angle, we must transform the attitude error angle in (34) into the mathematical platform misalignment angle so that it could be used as measurement. The conversion relation follows:

$$\phi = M \cdot \delta a \quad (35)$$

wherein, M is the conversion matrix of attitude error angle, as shown below. Let $\phi = [\phi_x \quad \phi_y \quad \phi_z]^T$ be the mathematical platform misalignment angle vector.

$$M = \begin{bmatrix} -\cos\psi & -\cos\theta\sin\psi & 0 \\ \sin\psi & -\cos\theta\cos\psi & 0 \\ 0 & -\sin\theta & 1 \end{bmatrix}$$

After conversion, ϕ is used as the observation of system attitude angle error and then the system measurement model is built as:

$$Z(t) = \begin{bmatrix} \phi_x \\ \phi_y \\ \phi_z \end{bmatrix} = HX(t) + V(t) \quad (36)$$

wherein, $H = [I_{3 \times 3} \quad 0_{3 \times 3} \quad 0_{3 \times 9}]$, $V = \begin{bmatrix} \Delta X_s \\ \Delta Y_s \\ \Delta Z_s \end{bmatrix}$, $\Delta X_s, \Delta Y_s, \Delta Z_s$ are the measurement noises of star sensor.

IV. SIMULATIONS AND RESULTS

This paper has studied the attitude estimation algorithm for the star-sensor aided GFSINS integrated navigation system. In order to verify that the UKF algorithm is superior to EKF, the same parameters should be set for system simulation in each group of comparative analysis. The initial conditions of simulation were set up as: 1)initial angular velocity was set to $0^\circ/s$; 2)the standard deviation of star-sensor measurement noise $\sigma_s = 5''$ and 3)the standard deviation of white noise disturbance torque $\sigma_{\Delta T} = 5 \times 10^{-3} N \cdot m$.

Computer simulation was implemented according to the corresponding parameters and initial conditions. The simulation results are shown in Fig. 4 - Fig. 6.

As can be seen from the figures, the size of initial deviation affects the time length of filtering convergence when sampling time is the same. That is, the smaller the initial deviation is, the faster the attitude error converges. Correspondingly, when the initial deviation is the same, the smaller the sampling time is, the shorter the filtering convergence time is, and the higher the accuracy of attitude convergence results will be. This is mainly because the smaller the sample

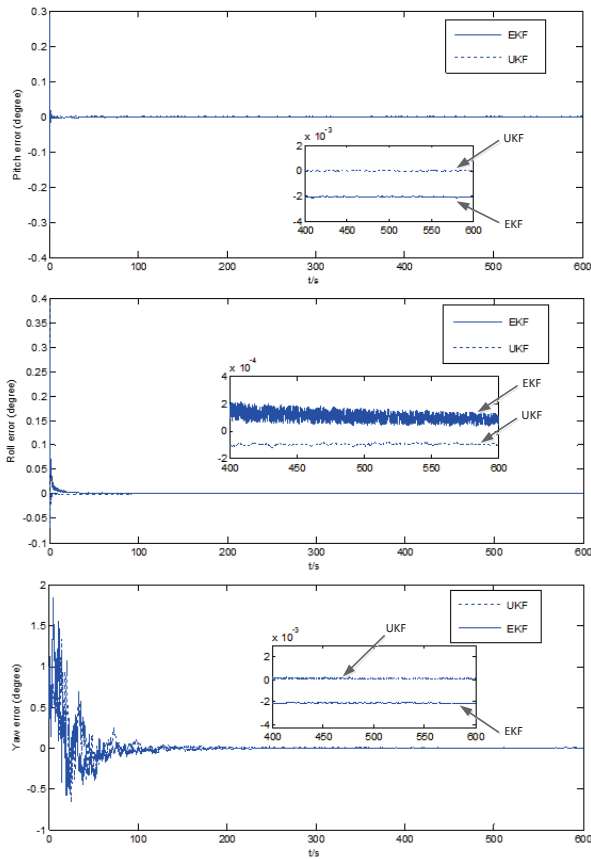


Fig. 4. Attitude Estimation Error (a. sampling time is 0.5s; initial attitude angle estimation are $\hat{\phi}(0) = 0.5^\circ$, $\hat{\theta}(0) = 0.5^\circ$, $\hat{\gamma}(0) = 1^\circ$.)

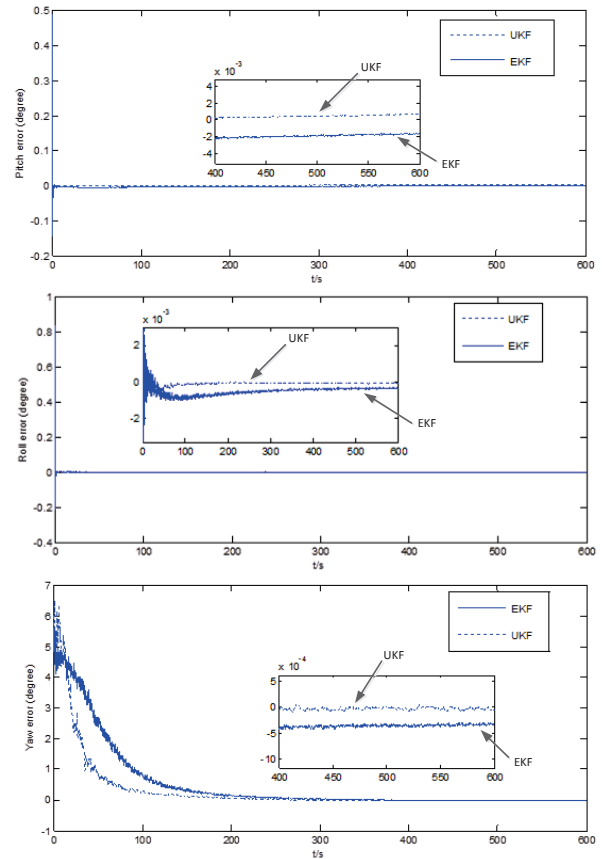


Fig. 6. Attitude Estimation Error (c. sampling time is 1s; initial attitude angle estimation are $\hat{\phi}(0) = 1^\circ$, $\hat{\theta}(0) = 1^\circ$, $\hat{\gamma}(0) = 5^\circ$.)

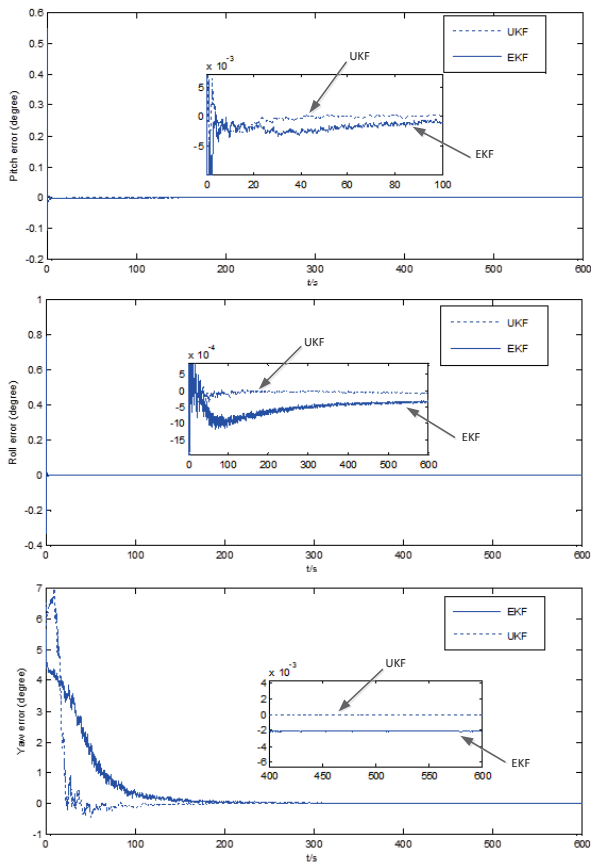


Fig. 5. Attitude Estimation Error (b. sampling time is 0.5s; initial attitude angle estimation are $\hat{\phi}(0) = 1^\circ$, $\hat{\theta}(0) = 1^\circ$, $\hat{\gamma}(0) = 5^\circ$.)

interval is, the shorter the filtering convergence time is, and the more timely the correction of attitude estimation can be obtained. In this way, it can also improve the attitude precision and reduce the vibration amplitude at the initial stage of filtering.

By contrasting the three groups of simulation figures, for nonlinear system, it is apparent that the accuracy of the mean and covariance estimated by using UKF algorithm is higher than that obtained by EKF. And both stability and precision of UKF are better than EKF. Furthermore, UKF is free from the computational complexity of Jacobi matrix, thus greatly improving the calculation speed. In addition, compared with EKF, UKF is more suitable for large misalignment task for GFSINS/star-sensor integrated navigation system.

V. CONCLUSION

GFSINS receives much concern in navigation field because of its particular advantages. In this research, the absolute value method is adopted to improve the accuracy of angular velocity calculation. Considering that the navigation error of GFSINS accumulates over time, the high precision attitude output of star sensor is used as aided information to correct the system. This paper carefully compares UKF with EKF concerning the attitude estimation of integrated navigation system. We conclude that, for nonlinear system (especially the complex), compared with EKF, UKF algorithm could improve the steady-state accuracy and convergence speed to a certain extent, and greatly increase the computation efficiency of the system. The proposed UKF attitude estimation

algorithm will be widely applied in the field of GFSINS/star-sensor integrated navigation.

REFERENCES

- [1] X. P. Zhao, T. Liu and D. Pan, "Improved method of restraining taper error in GFSINS[C]," in *IEEE International Conference on Electronic Measurement & Instruments*, pp. 330-335, 2015.
- [2] Q. N. Han, Y. L. Hao, Z. P. Liu and R. Wang, "Prediction of the angular velocity of GFSINS by BP neural network," *Journal of Huazhong University of Science & Technology*, vol. 39, no. 3, pp. 115-119, 2011.
- [3] Q. Li, Y. Y. Ben, Z. J. Zhu and J. L. Yang, "A Ground Fine Alignment of Strapdown INS under a Vibrating Base," *Journal of Navigation*, vol. 66, no. 1, pp. 49-63, 2013.
- [4] U. Nusbaum and I. Klein, "Feature article: Control theoretic approach to gyro-free inertial navigation systems," *IEEE Aerospace & Electronic Systems Magazine*, vol. 32, no. 8, pp. 38-45, 2017.
- [5] Q. Y. Wu, Q. Z. Jia, J. Y. Shan and X. Y. Meng, "Angular velocity estimation based on adaptive simplified spherical simplex unscented Kalman filter in GFSINS," *Proceedings of the Institution of Mechanical Engineers Part G Journal of Aerospace Engineering*, vol. 228, no. 8, pp. 1375-1388, 2014.
- [6] Z. Qi and Q. Y. Wang, "Error Analysis and the Development of an Error Mitigation Approach for Use in the Rotation Fiber Optic Gyro Inertial Navigation System," *Engineering Letters*, vol. 21, no. 4, pp. 203-211, 2013.
- [7] L. Y. Shi, K. Li and L. Chen, "Research on Passive Radar Guidance Head/GFSINS Integrated Navigation against Target Radar Shutdown Based on AUKF[C]," in *International Conference on Electrical, Computer Engineering and Electronics*, 2015.
- [8] M. Yang, M. Liu and D. Yang, "Research on the GFSINS/GPS/CNS integrated navigation technology for hypersonic vehicle[C]," in *Aiaa International Space Planes and Hypersonics Technologies Conference*, 2017.
- [9] L. F. Zhou, X. M. Zhao, S. Zhao, Q. Yao and L. Yang, "Initial alignment of CNS/INS integrated navigation system based on recursive least square method," *Journal of Chinese Inertial Technology*, vol. 23, no. 3, pp. 281-286, 2015.
- [10] N. Luo, L. Zhou, R. Zhang and J. W. Fan, "Research on CNS/SINS Integrated Navigation by Simulation," *Modern Navigation*, 2014.
- [11] C. Hajiyev, D. Cilden and Y. Somov, "Gyro-free attitude and rate estimation for a small satellite using SVD and EKF," *Aerospace Science & Technology*, vol. 55, pp. 324-331, 2016.
- [12] Q. Y. Wu, J. Y. Shan and S. B. Ni, "Application of Adaptive Unscented Kalman Filter for Angular Velocity Calculation in GFSINS[C]," in *Proceedings of International Conference on Modelling, Identification & Control. IEEE*, pp. 1305-1310, 2012.